EUROGRAPHICS 2001 / A. Chalmers and T.-M. Rhyne
(Guest Editors)

Volume 20 (2001), Number 3

Modeling Dynamic Hair as a Continuum

Sunil Hadap and Nadia Magnenat-Thalmann

{sunil,nadia}@miralab.unige.ch
MIRALab, CUI, University of Geneva, Switzerland
http://www.miralab.unige.ch/

Abstract

In this paper we address the difficult problem of hair dynamics, particularly hair-hair and hair-air interactions. To model these interactions, we propose to consider hair volume as a continuum. Subsequently, we treat the interaction dynamics to be fluid dynamics. This proves to be a strong as well as viable approach for an otherwise very complex phenomenon. However, we retain the individual character of hair, which is vital to visually realistic rendering of hair animation. For that, we develop an elaborate model for stiffness and inertial dynamics of individual hair strand. Being a reduced coordinate formulation, the stiffness dynamics is numerically stable and fast. We then unify the continuum interaction dynamics and the individual hair's stiffness dynamics.

1. Introduction

One of the many challenges in simulating believable virtual humans and animals has been to produce realistic looking hair. Hair simulation can be thought of having three different subtasks - shape modeling, dynamics and rendering. We can even classify the hair modeling attempts based on their underlying models, namely explicit hair models, cluster hair models and volumetric textures. Hair rendering and shape modeling of fur like short hair is becoming increasingly available to animators. However, shape modeling and dynamics of long hair has been difficult. The difficulties stem from the shear number of hair strands, their geometric intricacies and associated complex physical interactions. In this paper, we concentrate on the dynamics of long hair. The specific contributions are as follows:

- We address the problem of hair-hair, hair-body and hair-air interactions. We make a paradigm shift and model these interactions, in a unified way, as fluid dynamics. We use smoothed particle hydrodynamics (SPH) [1, 2] as a numerical model.
- We give an elaborate model for the stiffness dynamics of individual hair. We treat a hair strand as a serial rigid multibody system. This reduced coordinate formulation eliminates stiff numerical equations as well as enables a parametric definition of bending and torsional dynamics.

The detailed discussion on the state of the art in hair simulation can be found in [3]. Here, we limit the overview to the previous hair dynamics attempts, mainly explicit hair models. In these models, each hair strand is considered for shape and dynamics. That makes explicit models tedious for shape modeling and numerically intensive for dynamics, however they are intuitive and close to reality. They are especially suitable for dynamics of long hair. Daldegan *et al* [4] and Rosenblum *et al* [5] used a mass-spring-hinge model to control the position and orientation of hair strand. As their dynamic models were for straight hair, they could not be applied in animating hairstyles. Anjyo *et al* [6] modeled hair with a simplified cantilever beam and used one-dimensional projective differential equation of angular momentum to animate hair. Although the algorithm dealt with both hairstyling and hair animation, it had several limitations, the original hairstyle could not be recovered after subsequent animation and the movement of head was not accounted for. Further, the approximation in collision detection could generate unnatural results when the algorithm was used to animate long hair. To reduce computations, Daldegan *et al* [4] used a wisp model. Recently, Lee *et al* [7] developed on Anjyo's work to add some details to model hairstyles.

Appreciably, none of the previous attempts considered hair-hair and hair-air interactions. Even individual hair dynamics was grossly approximated to suit available computational power. However, in recent years the computing power has grown many times. Supercomputing power of the past is becoming increasingly available to animator's workstations. There is a need to develop new hair

Figure 1: *Hair as a Continuum*

dynamics models in light of current and future computing advances.

In the next section, we develop the basic continuum hair model. Section 3 gives a detailed model of stiffness dynamics for single hair. Section 4 explains the integration of two seemingly disparate approaches, hair volume as a continuum and dynamics of an individual hair. Section 5 extends the idea of hair as a continuum to a mixture of hair and air. Section 6 explains the implementation issues. Finally we show the results that demonstrate the effectiveness of the developed hair dynamics model in animating long hair.

2. Hair as a Continuum

Hair-hair interaction is probably the most difficult problem in achieving visually pleasing hair dynamics. So far, there are no good models developed in this regard. Though there are many advances in collision detection and response [8], they are simply unsuitable for the problem at hand, because of shear number complexity of hair. We take a radical approach by considering hair as a continuum. The continuum assumption states that the physical properties of a medium such as pressure, density and temperature are defined at each and every point in the specified region. Fluid dynamics regards liquids and gasses as a continuum and even elastic theory regards solids as such, ignoring the fact that they are still composed of individual molecules. Indeed, the assumption is quite realistic at a certain length scale of the observation but at smaller length scales the assumption may not be reasonable. One might argue, hair-hair spacing is not at all comparable to inter molecular distances to consider hair as a continuum. However, individual hair-hair interaction is of no interest to us apart from its end effect. Hence, we treat the size of individual hair and hair-hair distance much smaller than the overall volume of hair, justifying the continuum assumption. For an interesting discussion on the continuum assumption refer to [9]. As we develop the model further, it will be apparent that the above assumption is not just about approximating the complex hair-hair interaction. An individual hair is surrounded by air, as it moves it generate a boundary layer of air. This influences many other hair strands in motion. This aerodynamic form of friction is comparable to hair-hair contact friction. In addition, there are electrostatic forces to take part in the dynamics. It is not feasible to model these complex multiple forms of interactions. This inspires us to consider dynamics of single hair interacting with other surrounding hairs in a global manner through the continuum assumption. That way, we hope to have a sound model for an otherwise very complex phenomenon.

As we start considering hair as a continuum, we look at the properties of such a medium, namely the hair medium. There are two possibilities; hair medium could be considered as a solid or a liquid, depending on how it behaves under shearing forces. Under shearing stresses, solids deform till they generate counter stresses. If the shearing stresses are removed, the solids exhibit ability of retaining their original shape. The liquids are not able to withstand any shearing stresses. Under the influence of the shearing stresses they continue to deform indefinitely and they don't have any shape memory. In case of hair, if we apply a lateral shearing motion it acts like a liquid. At the same time, length wise, it acts as a solid. Thus there is a duality in the behaviour of hair as a continuum.

However, from an animation point of view, we cannot treat hair solely as a continuum, unless the viewpoint is far enough and individual hair movement is not perceived. Thus, we have to retain the individual character of hair as well, while considering hair as a continuum. We split hair dynamics into two parts:

- Hair-hair, hair-body and hair-air interactions, which are modeled using continuum dynamics, and more precisely fluid dynamics
- Individual hair geometry and stiffness, which is modeled using the dynamics of an elastic fiber

Interestingly, this approach even addresses the solid-liquid duality effectively. The model can be visualized as a bunch of hair strands immersed in a fluid. The hair strands are kinematically linked to fluid particles in their vicinity. The individual hair has its own stiffness dynamics and it interacts with the environment through the kinematical link with the fluid. Density, pressure and temperature are the basic constituents of fluid dynamics. The density of the hair medium is not precisely the density of individual hair. It is rather associated with the number density of hair in an elemental volume. In figure 1, observe that the density of hair medium is less when the number density of hair is less. The density of the hair medium is thus defined as the mass of the hair per unit occupied volume and is denoted as ρ. The notion of density of hair medium enables us to express the conservation of mass (it is rather conservation of the number of hair strands) in terms of the continuity equation [9]:

$$\frac{1}{\rho}\frac{d\rho}{dt} = -\nabla \cdot \vec{v} \tag{1}$$

where, $\vec{v}$ is the local velocity of the medium. The continuity equation states that the relative rate of change of density ($\frac{1}{\rho}\frac{d\rho}{dt}$), at any point in the medium, is equal to the negative gradient of the velocity field at that point ($-\nabla\cdot\vec{v}$). This is the total outflux of the medium at that point. The physical interpretation of the continuity equation in our case is that, as the hair strands start moving apart, their number density, and hence the density of the hair medium drops and vice a versa.

The pressure and the viscosity in the hair medium represent all the forces due to various forms of interactions of hair strands described previously. If we try to compress a bunch of hair, it develops a pressure such that hair strands will tend to move apart. The viscosity would account for various forms of interactions such as hair-hair, hair-body and hair-air. These are captured in the form of the momentum equation [9] of a fluid.

$$\rho\frac{d\vec{v}}{dt} = \nu\nabla\cdot(\nabla\vec{v}) - \nabla p + F_{bd} \tag{2}$$

The acceleration of fluid particles $\frac{d\vec{v}}{dt}$ with spatial pressure variation $-\nabla p$ would be such that it will tend to even out the pressure differences and as the fluid particles move, there will be always resistance $\nu\nabla\cdot(\nabla\vec{v})$ in the form of the friction. The body forces F_{bd}, *i.e.* the inertial forces and gravitational influence are also accounted for in the equation.

Temperature considerably affects the properties of hair. However, we do not have to consider it in dynamics. We treat the hair dynamics as an isothermal process unless we are trying to simulate a scenario of hair being dried with a hair dryer. Secondly, the temperature is associated with the internal energy of the fluid, which is due to the continuous random motion of fluid molecules. At the length scale of our model *i.e.* treating hair as a continuum, there is no such internal energy associated with the hair medium. Subsequently, we drop the energy equation of fluid, which is associated with the temperature and the internal energy.

The equation of state (EOS) [9] binds together all the fluid equations. It gives a relation between density, pressure and temperature. In our case of hair-hair interaction, EOS plays a central role along with the viscous fluid forces. The medium we are modeling is not a real medium such as gas or liquid. Hence, we are free to "design" EOS to suit our needs:

$$p = \begin{cases} 0 & \text{if } \rho < \rho_0, \\ K_c\left(\frac{\rho-\rho_0}{\rho_c-\rho_0}\right)^n & \text{if } \rho_0 \le \rho < \rho_c, \\ K_c & \text{if } \rho_c < \rho \end{cases} \tag{3}$$

We define hair rest density ρ_0 as a density below which statistically there is no hair-hair collision. In addition, we define hair close packing density as ρ_c that represents the state of the hair medium in which hair strands are packed to the maximum extent. This density is slightly lower than the physical density of hair, ρ_h. Figure 2 illustrates the relation between the density and the pressure of the hair medium. In the proposed pressure/density relationship, notice that there is no pressure built up below the hair rest density ρ_0. As one starts squeezing the hair volume, pressure starts building up. As a consequence, the hair strands are forced apart. At the hair compaction density ρ_c, the pressure is maximum. K_c is the compressibility of the hair volume. The power n refers to the ability of hair volume to get compressed. If the hair is well aligned, the power is high. As we compress the hair volume, suddenly hair strands start to form close packing and build the pressure quickly. On the contrary, if hair is wavy and not very well aligned, the pressure build up is not abrupt.

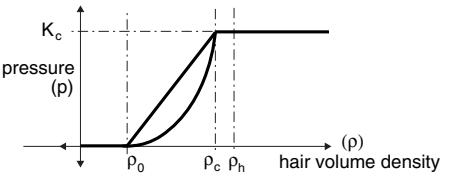

Figure 2: *Equation of State*

Instead of modeling collisions of individual hair strand with the body, we model them, in a unified way, as boundary condition of the fluid flow. There are two forms of fluid boundary conditions

- Flow tangency condition - The fluid flow normal to the obstacle boundary is zero
- Flow slip condition - The boundary exerts a viscous pressure proportional to the tangential flow velocity

Formulation of the flow boundary condition is deferred to section 4.

3. Single Hair Dynamics

In the previous section we discussed how we could think of hair-hair interaction as fluid forces by considering hair volume as a continuum. However, for the reasons explained there, we still need to retain the individual character of a hair strand. The stiffness dynamics of an individual hair is discussed in this section.

In a very straightforward manner, one may model hair as a set of particles connected by tensile, bending and torsional springs [4, 5], as shown in figure 3. If the hair strand is approximated by a set of n particles, then the system has $6n$ degrees of freedoms (DOFs) attributed to three translations, two bendings and one twist per particle. Treating each particle as a point mass, we can setup a set of governing differential equations of motion and try integrating them.

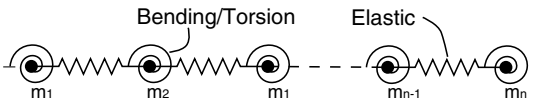

Figure 3: *Hair Strand as an Oriented Particle System*

Unfortunately this is not a viable solution. Hair is one of the many interesting materials in nature. It has remarkably high Elastic Modulus of 2-6GPa. Moreover, being very small in diameter, it has very large tensile strength when compared to its bending and torsional rigidity. This proves to be more problematic in terms of the numerics. We are forced to choose very small time steps due to the stiff equations corresponding to the tensile mode of motion, in which we are hardly interested. In fact, the hair fiber hardly stretches by its own weight and body forces. It just bends and twists.

Hence, it is better to choose one of the following two possibilities. Constrain the differential motion of the particles that amounts to the stretching using *constrained dynamics* [10]. Alternatively, reformulate the problem altogether to remove the DOFs associated with the stretching, namely a *reduced coordinate formulation* [11]. Both methods are equally efficient, being linear time. Parameterizing the system DOFs by an exact number of generalized coordinates may be extremely hard or even impossible for the systems having complex topology. In this case, a constrained method is preferred for its generality and modularity in modeling complex dynamical systems. However, for the problem at hand, the reduced coordinate formulation is a better method for the following reasons:

- Reduced coordinates are preferred when in our case the $3n$ DOFs remaining in the system are comparable to the $3n$ DOFs removed by the elastic constraints.
- The system has fixed and simple topology where each object is connected to maximum of two neighbours. We can take advantage of the simplicity and symbolically reduce the most of the computations.
- Reduced coordinate formulation directly facilitates the parametric definition of bending and torsional stiffness dynamics.

Subsequently we model an individual hair strand as a *serial rigid multibody chain*.

3.1. Hair as Serial Rigid Multibody Chain

The first step is to clearly define the serial rigid multibody system that approximates the motion of individual hair strand. We divide the strand into n segments of equal length. The advantages of defining segments of equal length will be made clear, subsequently. The segment length l may vary

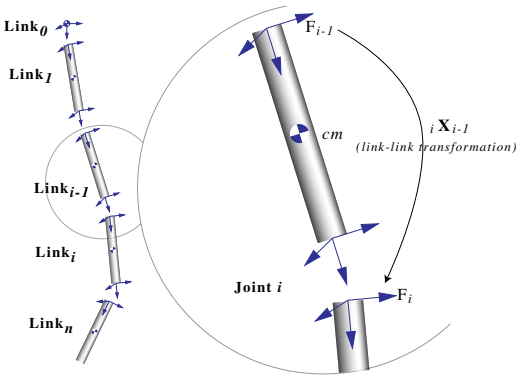

Figure 4: *Hair Strand as Rigid Multibody Serial Chain*

from strand to strand. The n segments are labelled as $link_1$ to $link_n$. Each link is connected to two adjacent links by a three DOF spherical joint forming a single un-branched open-loop kinematic chain. The joint between $link_{i-1}$ and $link_i$ is labelled $joint_i$. The position where the hair is rooted to scalp is synonymous to $link_0$ and the joint between head and hair strand is $joint_1$.

Further, we introduce n coordinate frames $\mathfrak{F}_i$, each attached to the corresponding $link_i$. The coordinate frame $\mathfrak{F}_i$ moves with the $link_i$. The choice of coordinate system is largely irrelevant to the mathematical formulations, but they do have an important bearing on efficiency of computations, which is discussed in Section 6. Having introduced the link coordinates, we need to be able to transform representations of the entities into and out of the link coordinates. ${}_i\hat{\mathbf{X}}_{i-1}$ is an adjacent-link coordinate *spatial transformation*[†] which operates on a *spatial vector* represented in coordinate frame $\mathfrak{F}_{i-1}$ and produces a representation of the same spatial vector in coordinate frame $\mathfrak{F}_i$. ${}_i\hat{\mathbf{X}}_{i-1}$ is composed of a pure translation, which is constant, and a pure orientation which is variable. We use a unit quaternion $\mathbf{q}_i$ to describe the orientation. Then, we augment components of n quaternions, one per joint, to form $\mathbf{q} \in \Re^{4n}$, the system state vector. Note that, additional n unit quaternion constraints, *i.e.* $|\mathbf{q}_i| = 1$, make system have $3n$ coordinates. Thus system is optimally represented to have $3n$ DOFs. Moreover, the angular velocity across the spherical joint is described by conventional 3×1 angular velocity vector $\mathbf{w}_i$. These form $\mathbf{w} \in \Re^{3n}$, the derivative state vector of the system.

The spatial motion of the rigid body, $link_i$ in our case, is fully characterized by its 6×1 *spatial velocity* $\hat{\mathbf{v}}_i$, 6×1 *spatial acceleration* $\hat{\mathbf{a}}_i$ and 6×6 *spatial inertia tensor* $\hat{\mathbf{I}}_i$. Figure 4 illustrates the definition of a hair strand as a serial multibody rigid chain.

[†] For discussion on spatial vector algebra refer [11].

3.2. Kinematic Equations

A 6×3 motion sub-space $\hat{\mathbf{S}}$ relates the angular velocity $\mathbf{w}_i$ to spatial velocity across the joint, which is the only allowed motion by the spherical joint. Since the position of the link in its own coordinate frame remains fixed, we can express the spatial inertia $\hat{\mathbf{I}}_i$ and the motion sub-space $\hat{\mathbf{S}}$ as a constant. Further, by proper choice of coordinate system, $\hat{\mathbf{I}}_i$ assumes a rather simple form. Subsequently, the velocity and acceleration across the spherical joint are given by the following equations:

$$\hat{\mathbf{v}}_i = {}_i\hat{\mathbf{X}}_{i-1}\hat{\mathbf{v}}_{i-1} + \hat{\mathbf{S}}\mathbf{w}_i \quad (4)$$

$$\hat{\mathbf{a}}_i = {}_i\hat{\mathbf{X}}_{i-1}\hat{\mathbf{a}}_{i-1} + \hat{\mathbf{v}}_i \hat{\times} \hat{\mathbf{S}}\mathbf{w}_i + \hat{\mathbf{S}}\dot{\mathbf{w}}_i \quad (5)$$

$$\hat{\mathbf{S}} = \begin{bmatrix} 1 & 0 & 0 \\ 0 & 1 & 0 \\ 0 & 0 & 1 \\ 0 & 0 & 0 \\ 0 & 0 & 0 \\ 0 & 0 & 0 \end{bmatrix}$$

Equations 4 and 5 enable us to recursively compute the link velocities $\hat{\mathbf{v}}_i$ and the link accelerations $\hat{\mathbf{a}}_i$, starting from $\hat{\mathbf{v}}_0$ and $\hat{\mathbf{a}}_0$, given joint angular velocities $\mathbf{w}_i$ and joint angular accelerations $\dot{\mathbf{w}}_i$. In our case $\hat{\mathbf{v}}_0$ and $\hat{\mathbf{a}}_0$ are the spatial velocity and the spatial acceleration of hair root, *i.e.* the scalp. We need to successively integrate the derivative vectors of the system *i.e.* $\dot{\mathbf{w}}_i$ and $\mathbf{w}_i$ to $\mathbf{w}_i$ and $\mathbf{q}_i$ respectively. The following equation relates the joint variable rates $\dot{\mathbf{q}}_i$ expressed as quaternions to the angular velocities $\mathbf{w}_i$

$$\begin{bmatrix} \dot{q}_0 \\ \dot{q}_1 \\ \dot{q}_2 \\ \dot{q}_3 \end{bmatrix} = 1/2 \begin{bmatrix} -q_1 & -q_2 & -q_3 \\ q_0 & -q_3 & q_2 \\ q_3 & q_0 & -q_1 \\ -q_2 & q_1 & q_0 \end{bmatrix} \begin{bmatrix} w_1 \\ w_2 \\ w_3 \end{bmatrix} \quad (6)$$

$$q_0^2 + q_1^2 + q_2^2 + q_3^2 = 1 \quad (7)$$

Next step is to identify various external forces acting on the links, which induce the joint angular accelerations and make hair strand bend and move.

3.3. Forward Dynamics of Hair Strand

A number of forces act on each link apart from the gravitational influence $\hat{\mathbf{g}}$. The explicit definition of the point of action of the spatial force on link is irrelevant as it is embedded in the definition of the spatial force.

- The gravitational influence is accommodated by giving the base a fictitious additional negative gravitational acceleration, *i.e.* by subtracting $\hat{\mathbf{g}}$ from $\hat{\mathbf{a}}_0$.
- Force $\hat{\mathbf{f}}_{ci}$ is the interaction spatial force (aggregate of line force and torque) on $link_i$ coming from the kinematic link with the hair medium as discussed in Section 2. The actual form of $\hat{\mathbf{f}}_{ci}$ is given in Section 4 and 5. This force accounts for all the interaction effects such as hair-hair collision, hair-body collision and hair-air drag.

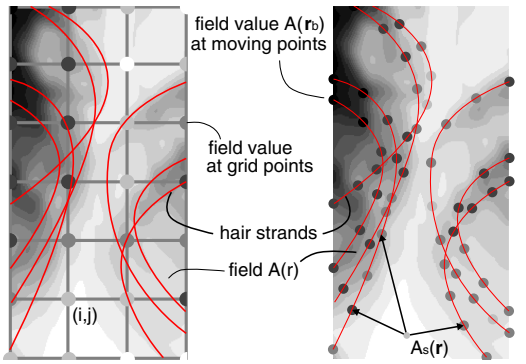

Figure 5: *Fluid Dynamics - Eulerian and Langrangian viewpoints*

- In order to account for the bending and torsional rigidity of the hair strand, the $joint_i$ exerts an actuator force $\mathbf{Q}_i^a \in \Re^3$ on both $link_{i-1}$ and $link_i$ in opposite directions. The actuator force is not a spatial force but rather a force expressed in joint motion space. The joint actuator force is a function of joint variables $\mathbf{q}_i$ incorporating the bending and torsional stiffness constants.

Given the set of forces acting on the system, we now need to calculate the induced joint angular accelerations $\dot{\mathbf{w}}_i$. This is a forward dynamics problem involving a rigid multibody system. We use Articulated-Body Method to solve the hair strand forward dynamics. This method has a computational complexity of $O(n)$. The detailed discussion of this algorithm is beyond the scope of this paper. It is comprehensively covered in [11, 12].

4. Fluid Hair Model

Establishing the kinematical link between the individual hair dynamics and the dynamics of interactions is a crucial part of the algorithm, which is done in this section.

The conventional fluid dynamics formulation uses Eulerian viewpoint. One way to think of Eulerian method is to think of an observer watching the fluid properties such as density, temperature and pressure change at a certain fixed point in space, as fluid passes through this point. In the numerical simulations, the space is discretised using a rectangular grid or a triangular mesh to define these few observation points for computations. Hence using the Eulerian viewpoint, we will ultimately get fluid forces acting at this fixed set of points. We would like to transfer the fluid force at each of these points onto the individual hair, which is in the vicinity of the point. There is no trivial correlation between the grid points and the hair strands, unless they coincide. Also the hair strand will be in the vicinity of new set of grid points every time it moves. This makes it difficult to formulate the kinematical link between the two. There are methods such as the particle-in-cell method, which try to do

the same. However, we opted for the other, less popular but effective, Langrangian formulation of fluid dynamics.

In Langrangian formulation, the physical properties are expressed as if the observer is moving with the fluid particle. *Smoothed Particle Hydrodynamics* (SPH) [2] is one of the Langrangian numerical methods, that utilizes space discretisation via number of discrete points that move with the fluid flow. One of the first applications of SPH in computer animation was done by Gascuel *et al* [1]. For a good overview of SPH, refer [13].

Figure 5 illustrates the concept of smoothed particles. The physical properties are expressed at the centre of each of these smoothed particles. Then the physical property at any point in the medium is defined as a weighted sum of the properties of all the particles.

$$A_s(\mathbf{r}) = \sum_b A_b \frac{m_b}{\rho_b} W(\mathbf{r} - \mathbf{r}_b, h) \tag{8}$$

The summation interpolant $A_s(\mathbf{r})$ can be thought of as the smoothed version of the original property function $A(\mathbf{r})$. The field quantities at particle b are denoted by a subscript b. The mass associated with particle b is m_b and density at the centre of the particle b is ρ_b, and the property itself is A_b. We see that the quantity $\frac{m_b}{\rho_b}$ is the inverse of the number density (*i.e.* the specific volume) and is, in some sense, a volume element.

To exemplify, the smoothed version of density at any point of medium is

$$\rho(\mathbf{r}) = \sum_b m_b W(\mathbf{r} - \mathbf{r}_b, h) \tag{9}$$

Similarly, it is possible to obtain an estimate of the gradient of the field, provided W is differentiable, simply by differentiating the summation interpolant

$$\nabla A_s(\mathbf{r}) = \sum_b A_b \frac{m_b}{\rho_b} \nabla W(\mathbf{r} - \mathbf{r}_b, h) \tag{10}$$

The interpolating kernel $W(\mathbf{r} - \mathbf{r}', h)$ has the following properties

$$\int W(\mathbf{r} - \mathbf{r}', h) d\mathbf{r}' = 1 \tag{11}$$

$$\lim W(\mathbf{r} - \mathbf{r}', h) = \delta(\mathbf{r} - \mathbf{r}') \tag{12}$$

The choice of the kernel is not important in theory as long as it satisfies the above kernel properties. For practical purposes we need to choose a kernel, which is simple to evaluate and has compact support. The *smoothing length* h defines the extent of the kernel. We use the cubic spline interpolating kernel.

$$W(\mathbf{r}, h) = \frac{\sigma}{h^\nu} \begin{cases} (1 - \frac{3}{2}s^2 + \frac{3}{4}s^3) & \text{if } 0 \le s \le 1, \\ \frac{1}{4}(2-s)^3 & \text{if } 1 \le s \le 2, \\ 0 & \text{otherwise} \end{cases} \tag{13}$$

Where $s = |\mathbf{r}|/h$, ν is the number of dimensions and σ is the normalization constant with values $\frac{2}{3}$, $\frac{10}{7\pi}$, or $\frac{1}{\pi}$ in one, two, or three dimensions, respectively. We can see that the kernel has a compact support, *i.e.* its interactions are exactly zero at distances $|\mathbf{r}| > 2h$. We keep the h constant throughout the simulation to facilitate a speedy search of neighbourhood of the particles. The nearest neighbour problem is well known in computer graphics. Section 6 gives the strategy for the linear time neighbour search.

There is no underlying grid structure in the SPH method, which makes the scheme suitable for our purpose. We are free to choose the initial positions of the smoothed particles as long as their distribution reflects the local density depicted by Equation 9. Eventually the particles will move with the fluid flow. In order to establish the kinematical link between the individual hair dynamics and the dynamics of interactions, we place the smoothed particles directly onto the hair strands as illustrated in the Figure 5. We keep the number of smoothed particles per hair segment constant, just as we have kept the hair segment length constant, for reasons of computational simplicity. As the smoothed particles are glued to the hair strand, they can no longer move freely with the fluid flow. They just exert forces arising from the fluid dynamics onto the corresponding hair segment and move with the hair segment (in the figure, the hair strand is not discretised to show the segments). Using this method, we have incorporated both, the elastic dynamics of individual hair and the interaction dynamics into hair dynamics.

Apart from providing the kinematical link, the SPH method has other numerical merits when compared to a grid-based scheme:

- As there is no need for a grid structure, we are not defining a region of interest to which the dynamics must confine to. This is very useful considering the fact that, in animation the character will move a lot and the hair should follow it.
- No memory is wasted in defining field in the region where there is no hair activity, which is not true in the case of grid-based fluid dynamics.
- As the smoothed particles move with the flow carrying the field information, they optimally represent the fluctuations of the field. In the case of grid-based scheme, it is necessary to opt for tedious adaptive grid to achieve similar computational resolution.

In the rest of the section, we discuss the SPH versions of the fluid dynamics equations. Each smoothed particle has a constant mass m_b. The mass is equal to the mass of the respective hair segment divided by the number of smoothed particles on that segment. Each particle carries a

variable density ρ_b, variable pressure p_b and has velocity $\mathbf{v}_b$. The velocity v_b is actually the velocity of the point on the hair segment where the particle is located, expressed in the global coordinates. $\mathbf{r}_b$ is the global position of the particle, *i.e.* the particle location on the hair segment in the global coordinates. Once initially we place the particles on the hair strands, we compute the particle densities using Equation 9. Indeed, the number density of hair at a location reflects the local density, which is consistent with the definition of the density of the hair medium given in Section 2.

For brevity, introducing notation $W_{ab} = W(\mathbf{r}_a - \mathbf{r}_b, h)$ and let $\nabla_a W_{ab}$ denote the gradient of W_{ab} with respect to $\mathbf{r}_a$ (the coordinates of particle a). Also quantities such as $\mathbf{v}_a - \mathbf{v}_b$ shall be written as $\mathbf{v}_{ab}$.

The density of each particle can be always found from Equation 9, but this equation requires an extra loop over all the particles (which means the heavy processing of nearest neighbour finding) before it can be used in the calculations. A better formula is obtained from the smoothed version of the continuity equation (equation 1).

$$\frac{d\rho_i}{dt} = \sum_{j=1}^{N} m_j \mathbf{v}_{ij} W_{ij} \tag{14}$$

We now can update the particle density without going through the particles just by integrating the above equation. However, we should correct the densities using Equation 9, to avoid the density being drifted.

The smoothed version of the momentum equation, Equation 2, without the body forces, is as follows

$$\frac{d\mathbf{v}_i}{dt} = -\sum_{j=1}^{N} m_j \left(\frac{p_j}{\rho_j^2} + \frac{p_i}{\rho_i^2} + \prod_{ij}\right) \nabla_i W_{ij} \tag{15}$$

The reason for dropping the body force F_{bd} is that, the comprehensive inertial and gravitational effects are already incorporated in the stiffness dynamics of the individual strand. Otherwise, we would be duplicating them.

As the particles are glued to the respective hair segment, they cannot freely achieve the acceleration $\frac{d\mathbf{v}_i}{dt}$ given by the momentum equation. Instead we convert the acceleration into force by multiplying it with the mass of the particle m_i. The force gets exerted ultimately onto the hair segment. In the previous section, we referred the total of all the fluid forces due to each particle on the segment as the interaction force $\hat{\mathbf{f}}_{ci}$. Although we need to convert the Cartesian form of forces into the spatial forces, this is straightforward.

In Equation 15, $\prod_{ij}$ is the viscous pressure, which accounts for the frictional interaction between the hair strands. We are free to design it to suit our purpose, as it is completely artificial viscosity, *i.e.* it has no relation to the viscous term $\nu\nabla\cdot(\nabla\vec{v})$ in the momentum equation (Equation 2). Taking inputs from the artificial viscosity form for SPH proposed by [13], we set it to

$$\begin{aligned} \prod_{ij} &= \begin{cases} \frac{-c\mu_{ij}}{\rho_{ij}} & \text{if } \mu_{ij} < 0 \\ 0 & \text{if } \mu_{ij} \geq 0 \end{cases} \\ \mu_{ij} &= h\frac{\mathbf{v}_{ij}\cdot\mathbf{r}_{ij}}{|\mathbf{r}_{ij}|^2 + h^2/100} \\ \bar{\rho}_{ij} &= (\rho_i + \rho_j)/2 \end{aligned} \tag{16}$$

The constant c is the speed of sound in the medium. However, in our case, it is just an animation parameter. We are free to set this to an appropriate value that obtains satisfactory visual results. The term incorporates both bulk and shear viscosity.

It is quite straightforward to model solid boundaries, either stationary or in motion, with special boundary particles. The boundary particles do not contribute to the density of the fluid and they are inert to the forces coming from the fluid particles. However, they exert a boundary force onto the neighbouring fluid particles. A typical form of boundary force is as given in [13]. Each boundary particle has an outward pointing unit normal $\mathbf{n}$ and exerts a force

$$\begin{aligned} \mathbf{f}_n &= f_1(\mathbf{n}\cdot\triangle\mathbf{r})P((t)\cdot\triangle\mathbf{r})\mathbf{n} \\ \mathbf{f}_t &= K_f(\mathbf{t}\cdot\triangle\mathbf{v})\mathbf{t} \end{aligned} \tag{17}$$

Where, $\mathbf{n}$ is outward normal at the boundary particle, $\mathbf{t}$ is the tangent. Function f_1 is any suitable function, which will repel the flow particle away. P is Hamming window, which spreads out the effect of the boundary particle to neighbouring points in the boundary. That way, we have a continuous boundary defined by discrete set of boundary particles. The coefficient of friction K_f defines the tangential flow slip force $\mathbf{f}_t$.

At each step of the integration, first we obtain the density at each particle ρ_i using Equation 14. To correct numerical errors from time to time, we use Equation 9. The only unknown quantity so far is the pressure at each particle p_i. Once we know the particle densities ρ_i, the equation of the state (Equation 3), directly gives the unknown pressures. This is the central theme of the algorithm. Subsequently, we compute the fluid forces acting on each particle using the momentum equation (Equation 15). We know now the interaction forces $\hat{\mathbf{f}}_{ci}$ for each hair segment and we are ready to integrate the equation of the motion for individual hair strand.

5. Hair-air, a mixture

So far we have not considered interaction of hair with air, we only considered hair-hair and hair-body interactions in sections 2 and 4. Hair-air interaction is important for the following reasons:

- The air drag is quite significant as the mass of an individual hair strand is very small compared to the skin friction drag created by the surface. Thus, most of the damping in hair dynamics comes from the air drag.
- We would like to animate hair blown by wind.
- Air plays a major role in hair-hair interaction. As a hair strand moves through air, it generates a boundary layer, which influences the neighbouring hair strand even if the physical contact is minimum.
- Most importantly, hair volume affects the air field. Hair volume is not completely porous. Thus it acts as a partial obstacle to the wind field, to alter it.

Initially we thought of a very simple model for adding wind effects in the hair animation. There are significant advances in computer graphics for modeling turbulent gaseous fields [14]. We added extra force to each of the smoothed particles $\hat{\mathbf{f}}_{di} = \mu(\hat{\mathbf{v}}_{wi} - \hat{\mathbf{v}}_i)$ in addition to the interaction force $\hat{\mathbf{f}}_{ci}$. Here, $\hat{\mathbf{v}}_{wi}$ is the local wind velocity at particle i, expressed in the spatial vector and $\hat{\mathbf{v}}_i$ is the velocity of the particle i. μ is the drag coefficient, which is an animation parameter. However, this strategy is a passive one. As mentioned in the last item above, hair volume should also affect the wind field for more realistic animations, as it is not completely porous.

Subsequently, we extend the hair continuum model. We postulate that the hair medium is a mixture of hair material and air. There are many ways to model a mixture; we model it in a very straightforward way. Let the two fluids, hair medium and air, have their own fluid dynamics. We just link the two by adding extra drag force to the momentum equation. Thus, the SPH forms of the equations for the hair-air mixture are:

$$\frac{d\rho_i^h}{dt} = \sum_{j=1}^{N} m_j^h (\mathbf{v}_i^h - \mathbf{v}_j^h) W_{ij} \quad \text{hair continuity} \qquad (18)$$

$$\frac{d\rho_k^w}{dt} = \sum_{l=1}^{M} m_l^w (\mathbf{v}_k^w - \mathbf{v}_l^w) W_{kl} \quad \text{air continuity} \qquad (19)$$

$$\frac{d\mathbf{v}_i^h}{dt} = \frac{\mu(\mathbf{v}^a(\mathbf{r}_i^h) - \mathbf{v}_i^h)}{m_i} - \sum_{j=1}^{N} m_j^h \left(\frac{p_j^h}{\rho_j^{h2}} + \frac{p_i^h}{\rho_i^{h2}} + \prod_{ij}^{h}\right) \nabla_i W_{ij} \qquad (20)$$

$$\frac{d\mathbf{v}_k^a}{dt} = \frac{\mu(\mathbf{v}^h(\mathbf{r}_k^a) - \mathbf{v}_k^a)}{m_k} - \sum_{l=1}^{M} m_l^a \left(\frac{p_l^a}{\rho_l^{a2}} + \frac{p_k^a}{\rho_k^{a2}} + \prod_{kl}^{a}\right) \nabla_k W_{kl} \qquad (21)$$

Observe that there are two different sets of smoothed particles corresponding to two constituents of the mixture. $\mathbf{v}^a(\mathbf{r}_i^h)$ is air velocity experienced by the hair particle i, *i.e.* the velocity estimate of air at point $\mathbf{r}_i^h$ and vice versa for the air particle. Thus there is a coupling by the drag coefficient μ between the two fluid dynamics.

6. Implementation

In this section we discuss some of the implementation issues.

6.1. Fast computation of single hair dynamics

Modeling a hair strand as a rigid multibody serial chain accurately captures all the relevant modes of motion and stiffness dynamics. Formulating only the exact number of relevant DOFs, *i.e.* bending and torsion, we have removed the source of the stiff equations of motion associated with the high tensile rigidity of the hair strand. Hence, we obtain an advantage in terms of possible large simulation time steps, even though the dynamics calculations are a bit involved.

We keep the length of the hair segment per hair strand constant. We also align the hair segment's local coordinate system to the principal inertial axis. That way the 6x6 spatial inertia tensor takes a simple form with many zeros and is constant. Length being constant, the only variable part in the coordinate transformation, from one link to another, is rotation. Exploiting the special multi-body configuration of hair, we have symbolically reduced most of the Articulated Rigid Body Dynamics calculations and have fine-tuned it to be most efficient. The time complexity of algorithm is linear. This puts no restriction on the number of rigid segments we can have per hair strand.

Finally, we parallelize the task of the hair strand computation. We exploit four-way parallel Single Instruction Multiple Data (SIMD) capability of Pentium III processors. We sort the hair strands by their number of hair segments. Then we club four hair strands, equal in number of segments, as far as possible or we trim a few. We then can compute four hair strands at a time on a single processor. Additionally, we assume two to four CPUs are available to use. Using these strategies, we are able to simulate 10,000 hair strands, having 30 segments on an average, in less than 2 minutes.

6.2. Efficient implementation of Smoothed Particle Hydrodynamics

The smoothed particle's kernel has compact support. The particle influences only its near neighbours, more precisely the ones that are in the circle of smoothing length. Thus the time complexity of the fluid computation is O(kn), where n is the total number of particles and k is the typical number of particles coming under influence of one particle. We still have to ensure that we use an efficient algorithm to locate the neighbours. There are many strategies for collision detection and neighbour search. For a detailed survey, refer to Lin and Gottschalk [8]. However, smoothed particles being point geometries, we use the Octree space partitioning. Vemuri *et al* [15] used the Octree for granular flow which is very similar to our application. We use fourth order Runge-Kutta integration method to integrate the dynamics.

7. Results

We report three animations using the described methodology. They are in increasing order of scene complexity. However, they utilize the same underlying models discussed so far. The simplest of the animations highlight a multitude of the dynamics in minute detail and the more complex ones illustrate the effectiveness of the methodology in animating real life hair animations.

- In the first animation, from the initial spread, individual hair strands collapse under gravity. Hair strands have their shape memory working against gravity. Otherwise they would have straightened up at frame 24. Also, as the hair strands get close, the pressure builds up due to increase in the number density in the "hair fluid", which further retains the volume, throughout the animation, by keeping individual hair apart. The inertial forces and the influence of air are evident in the oscillatory motion of hair. The air drag is most effective towards the tip of hair strands. Observe the differential motion between the tips. Hair strands on the periphery experience more air drag than the interior ones. This is only possible due to the fluid-hair mixture model; the movement of hair does set air in motion like a porous obstacle.
- The second animation scenario is to illustrate the "fluid" motion of hair without loosing the character of individual hair. The hair volume starts falling freely under gravity. Quickly, the individual hair's length constraint and stiffness restricts the free falling motion to give it a bounce, towards end of the free fall (frame 53). At the same time, "hair fluid" collides with the body and bursts away sidewise (frame 70). The air interaction gives an overall damping. Observe that the hair quickly settles down, even after the sudden jerk in the motion, due to air drag and hair friction with the body.
- The third animation exclusively illustrates the effectiveness of the model in animating hair blown by wind. Needless to say that there is an influence of airfield on individual hair. More importantly, body and hair volume acts as a full and partial obstacle to air altering its flow.

8. Acknowledgements

This work is partially supported by Swiss National Research Foundation (FNRS). Special thanks are due to Chris Joslin for proof reading this paper and to Prithweesh De for preparing the multimedia presentation.

References

1. J.D. Gascuel, M.P. Cani, M. Desbrun, E. Leroy, and C. Mirgon. Smoothed particles: A new paradigm for animating highly deformable bodies. In *6th Eurographics Workshop on Animation and Simulation'96*. Paris, September 1996. 1, 6
2. J. J. Monaghan. Smoothed particle hydrodynamics. *Annual Review of Astronomy and Astrophysics*, 30:543–574, 1992. 1, 6
3. Sunil Hadap and Nadia Magnenat-Thalmann. State of the art in hair simulation. In *Proceedings of International Workshop on Human Modeling and Animation*, pages 3–9, Seoul, Korea, June 2000. Korea Computer Graphics Society. 1
4. Agnes Daldegan, Nadia Magnenat Thalmann, Tsuneya Kurihara, and Daniel Thalmann. An integrated system for modeling, animating and rendering hair. *Computer Graphics Forum (Eurographics '93)*, 12(3):211–221, 1993. Held in Oxford, UK. 1, 3
5. Robert Rosenblum, Wayne Carlson, and Edwin Tripp. Simulating the structure and dynamics of human hair: Modeling, rendering and animation. *Journal of Visualzation and Computer Animation*, 2:141–148, June 1991. John Wiley. 1, 3
6. Ken ichi Anjyo, Yoshiaki Usami, and Tsuneya Kurihara. A simple method for extracting the natural beauty of hair. *Computer Graphics (Proceedings of SIGGRAPH 92)*, 26(2):111–120, July 1992. 1
7. Doo-Won Lee and Hyeong-Seok Ko. Natural hairstyle modeling and animation. In *Proceedings of International Workshop on Human Modeling and Animation*, pages 11–21, Seoul, Korea, June 2000. Korea Computer Graphics Society. 1
8. M. Lin and S. Gottschalk. Collision detection between geometric models: A survey. In *Proceedings of IMA Conference on Mathematics of Surfaces*, 1998. 2, 8
9. Ronald L. Panton. *Incompressible Flow*. John Wiley, 2nd edition edition, December 1995. 2, 3
10. David Baraff. Linear-time dynamics using lagrange multipliers. *Proceedings of SIGGRAPH 96*, pages 137–146, August 1996. 4
11. Roy Featherstone. *Robot Dynamics Algorithms*. Kluwer Academic Publishers, 1987. 4, 5
12. Brian Mirtich. *Impulse-based Dynamic Simulation of Rigid Body Systems*. PhD thesis, University of California, Berkeley, December 1996. 5
13. Joseph Peter Morris. An overview of the method of smoothed particle hydrodynamics. AGTM Preprints, University of Kaiserslautern, 1995. 6, 7
14. Jos Stam. Stochastic dynamics: Simulating the effects of turbulence on flexible structures. *Computer Graphics Forum*, 16(3):159–164, August 1997. 8
15. B. C. Vemuri, L. Chen, L. Vu-Quoc, X. Zhang, and O. Walton. Efficient and accurate collision detection for granular flow simulation. *Graphical Models and Image Processing*, 60(5):403–422, November 1998. 8

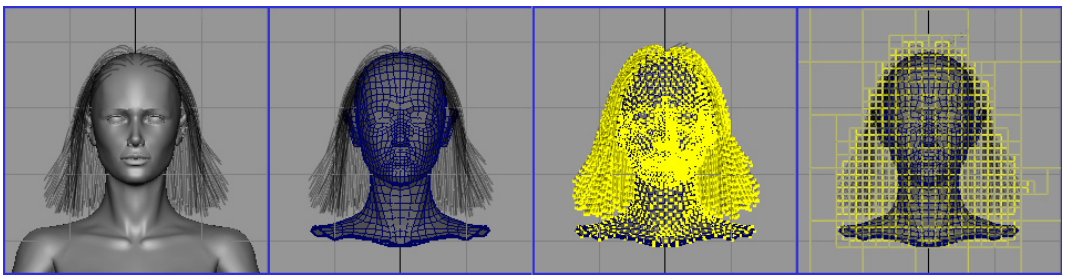

Figure 6: *Approximate geometry, Smoothed particles, Octree*